# Metallurgical Characterization of New Palladium-Containing CoCr and NiCr Alloys

Raghav Puri
*Marquette University*

# METALLURGICAL CHARACTERIZATION OF NEW PALLADIUM-CONTAINING CoCr AND NiCr ALLOYS

by

Raghav Puri, BDS

A Thesis submitted to the Faculty of the Graduate School,
Marquette University,
in Partial Fulfillment of the Requirements for
the Degree of Master of Science

Milwaukee, Wisconsin

May 2011

ABSTRACT
METALLURGICAL CHARACTERIZATION OF NEW PALLADIUM-CONTAINING CoCr AND NiCr ALLOYS

Raghav Puri, BDS

Marquette University, 2011

Recently introduced to the market has been an entirely new subclass of casting alloy composition whereby palladium (~25 wt%) is added to traditional base metal alloys such as CoCr and NiCr.

**Objectives:** The purpose of this study was to evaluate the microstructure and Vickers hardness of two new CoPdCr and one new NiPdCr alloy and compare them to traditional CoCr and NiCr alloys.

**Methods**: The casting alloys investigated were: CoPdCr-A (Noble Crown NF, The Argen Corporation), CoPdCr-I (Callisto CP+, Ivoclar Vivadent), NiPdCr (Noble Crown, Argen), CoCr (Argeloy N.P. Special, Argen), and NiCr (Argeloy N.P. Star, Argen). As-cast cylindrical alloy specimens were mounted in epoxy resin and prepared with standard metallographic procedures, i.e. grinding with successive grades of SiC paper and polishing with alumina suspensions. The alloys were examined with an optical microscope, SEM/EPMA, and XRD to gain insight into their microstructure, composition, and crystal structure. Vickers hardness (VHN) was measured and statistically analyzed by one way ANOVA and Tukey's HSD test ($\alpha$=0.05).

**Results:** Optical microscopy showed a dendritic microstructure for all alloys. The Pd-containing alloys appear to possess a more complex microstructure. SEM/ EPMA showed Cr to be rather uniformly distributed in the matrix with palladium tending to be segregated apart from Mo and Ni or Co. Areas of different composition may explain the poor electrochemical results noted in previous studies. XRD suggested the main phase in the Ni-containing solutions was a face centered cubic Ni solid solution, whereas the CoCr exhibited a hexagonal crystal structure that was altered to face centered cubic when Pd was included in the composition. For Vickers hardness, the Co-containing alloys possessed a greater hardness than the Ni-containing alloys. However, the incorporation of Pd in CoCr and NiCr had only a slight effect on microhardness.

**Conclusion:** Overall, the inclusion of palladium increases the microstructural complexity of NiCr and CoCr alloys.

# ACKNOWLEDGEMENTS

Raghav Puri, BDS


## To My Program Director

I would especially like to express my gratitude to my director, Dr. David W. Berzins, for his guidance and direction with this thesis. I am grateful for his patience, knowledge, support, and kindness with both this project and throughout my residency.

## To My Thesis Committee Member

I would also like to thank Dr. Gerald Ziebert, Dr. Jeffrey Toth, and Dr. Harshit Aggarwal for their contributions in making this thesis project a reality. I would also like to thank Dr. Isao Kawashima from Ohu University School of Dentistry in Kōriyama, Fukushima, Japan for assisting with the SEM/EPMA and XRD studies. I would also like to thank Drs. Kelly Beck and Demetri Sarantopoulos for help in making specimens.

## To My Parents

On a personal note, I want to thank my father Parmesh Puri and mother Pooja Puri, who have been the driving force for all my achievements. You gave me the foundation to become the person I am; without your confidence, pride, and encouragement I could never have overcome the challenges to attain this goal.

I would also like to deeply thank my brother Gaurav Puri and sister-in-law Gunjan Dhir for their love and unconditional support during the last 9 years, which has brought me to this day. I share this accomplishment with you.

To My Wife

My deepest Love and most sincere thanks go to my wonderful wife Deepa Verma. She has supported me with her extensive knowledge and her unfailing love.

Finally I would like to thank the Argen Corporation and Ivoclar Vivadent, Inc. for providing the casting alloys used in this thesis. Also, I thank Mr. Orville Colby of Capitol Dental Lab in Menomonee Falls, WI for casting the specimens.

At the end, I would like to acknowledge that there are many people to whom I am indebted.

TABLE OF CONTENTS

# LIST OF TABLES

# LIST OF FIGURES

# INTRODUCTION

Many different alloys have been used for fixed prosthodontic restorations. Factors such as cost, ease of casting and finishing, various mechanical properties such as hardness, elastic modulus, and yield strength, color, accuracy of fit, and worries about alloy corrosion have made selection of alloys complex. The American Dental Association (ADA) has classified alloys into 4 classes on the basis of composition: high noble, noble, and predominantly base metal alloys, in addition to titanium and titanium alloys.[1] Noble alloys are defined as having a noble metal (gold, platinum, palladium, rhodium, iridium, osmium, ruthenium) content greater than or equal to 25% by weight (wt%). Apart from the silver-palladium casting alloys, the other subclasses encompassing the noble alloy class in general contain significantly greater than 25 wt% noble metal.[2,3] On the other hand, the predominantly base metal class is defined as containing <25 wt% noble metal, but the base metal alloys typically contain no noble metals or at most, only a few wt%.

Recently introduced to the dental market have been cobalt-chromium (CoCr) or nickel-chromium (NiCr) based alloys with 25.0 wt% palladium (Pd) added (Callisto CP/Callisto CP+, Ivoclar Vivadent, Amherst, NY; NobleCrown and NobleCrown NF, The Argen Corporation, San Diego, CA). This represents an exclusively new subclass of casting alloy composition of noble alloys since the addition of palladium is just enough to classify them as such. Consequently, although they are noble alloys, they have a lower cost than noble gold-based alloys or high-palladium alloys (with 70-90% Pd), therefore making them potentially attractive on an economic basis to some clinicians and/or dental laboratories. Additionally, 75 wt% of the alloys are similar to CoCr or NiCr formulations which are relatively inexpensive. Unfortunately, little material property information is

available on these specific alloy systems except for some recently conducted research on their corrosion properties.[4,5]

The corrosion resistance of NiCr, as well as CoCr, alloys has been found to be related to their Cr and Mo content due to the formation of a surface passive film containing $Cr_2O_3$, $MoO_3$, and other oxides.[6] Still, the corrosion resistance of NiCr alloys has been found to be lower than gold and palladium-based alloys.[7] Specifically, Pd–based and AuPtPd dental alloys have been categorized as being the most resistant to electrochemical and chemical corrosion, even better than gold.[8] Thus, if palladium were introduced into CoCr or NiCr alloys, their corrosion resistance most likely would be expected to increase. However, Sarantopoulos et al. evaluated the corrosion properties of palladium-containing alloys and found that the incorporation of palladium had a detrimental effect on the corrosion properties of CoCr and NiCr casting alloys.[4] Micrographs of the corroded specimens showed localized areas of corrosion, leading the authors to speculate that microstructural features were responsible for the decreased corrosion resistance of the CoPdCr and NiPdCr alloys.

The microstructure of traditional CoCr and NiCr alloys has been evaluated by several researchers. For example, as is commonly observed, Wylie et al.[9] viewed a dendritic microstructure for two Ni-based alloys. Optical microscopy showed solute-rich interdendritic regions between the matrix and particle phases.[9] Others have examined oxidation effects. X-ray diffraction showed that oxides generated with low-temperature ($650^oC$) oxidation contained all of the elements in the composition, whereas NiO and $Cr_2O_3$ were predominant with high temperature oxidation (1000°C).[10] Also, it has been found that the distribution of Ni and Cr in the oxide layers varies with the alloy, and

oxidation in air results in thicker oxide layers than does oxidation in a reduced oxygen atmosphere.[10] Thus, the mechanisms of oxidation vary with temperature and alloy composition.[10] Another study found phase changes in some alloys occur due to the depletion of alloying elements in the matrix after oxidation treatments.[11]

Given that CoPdCr and NiPdCr alloys are relatively new, their microstructure and phase composition has not been documented. This information is important for the interpretation of corrosion behavior, mechanical properties, and ultimately clinical performance. The aim of this thesis was to evaluate the microstructure and phase composition of the 2 CoPdCr and 1 NiPdCr alloys and compare them to traditional CoCr and NiCr alloys.

# LITERATURE REVIEW

The metallurgy of alloys can be important for interpretation of microstructural observations, mechanical properties, corrosion behavior, and clinical performance. The overall goal of this research was to evaluate the metallurgical characteristics of 3 new casting alloys (2 CoPdCr and 1 NiPdCr) and compare them to existing CoCr and NiCr alloys. With this in mind, basic concepts regarding casting alloys and relevant literature on CoCr, NiCr, and palladium-based alloys will be reviewed next.

## Casting alloy basics

Castings are made by fabricating a hollow mould, pouring a molten metal/alloy into the mould, allowing the metal/alloy to solidify, and separating the solid metal from the mould. Dental casting alloys are used for inlays, onlays of all classes, as well as for individual partial- and full-coverage restorations and frameworks for fixed and removable partial dentures. ANSI/ADA Specification No. 5 for Dental Casting Alloys provides a classification and specifies requirements and test methods for dental casting alloys used in the fabrication of dental restorations and appliances. Cast dental alloys can be classified according to the following five types: (1) Use (such as all-metal inlays, crowns and bridges, metal-ceramic prostheses, posts and cores, removable partial dentures, and implants); (2) major elements (such as gold-based, palladium-based, silver-based, nickel-based, cobalt-based, titanium-based); (3) nobility (such as high noble, noble, predominantly base metal); (4) principal three elements (such as AuPdAg, PdAgSn, NiCrBe, CoCrMo, TiAlV, FeNiCr and ; (5) dominant phase system (such as single phase, eutectic, peritectic, and intermetallic).[12]

The ADA classifies alloys into 4 classes on the basis of composition: high noble alloys, noble alloys, and predominantly base metal alloys, in addition to titanium and titanium alloys.[1] High noble alloys have a gold content of ≥ 40 wt% and an overall noble metal (gold, palladium platinum, ruthenium, rhodium, iridium, and osmium) content of ≥ 60 wt%. Predominantly base alloys have a noble metal content of < 25 wt% whereas the titanium and titanium alloys class have titanium contents ≥ 85 wt%. Noble alloys are defined as having a noble metal content ≥ 25 wt%. Recognized subclasses of the noble alloy class include AuCuAgPd, PdAg, AgPd, and PdCu (or other "high palladium" groups (PdCo or PdGa).[2] Apart from the silver-palladium casting alloys, the other subclasses encompassing the noble alloy class in general contain significantly greater than 25 wt% noble metal. On the other hand, despite the predominantly base metal class being defined as containing <25 wt% noble metal, the base metal alloys (CoCr and NiCr) typically contain no noble metals or at most, only a few wt%.

**Alloys, phases, and microstructure**

Like aqueous solutions, liquid metals may mix together. Some metals are soluble in each other, while others are partially soluble ore even insoluble. Some metals, while in the molten state, will chemically react with others to form new chemical compounds, typically called intermetallic compounds. When two or more molten metals are mixed together and allowed to cool to a solid crystalline state, the result is called an alloy.

An alloy is a substance with metallic properties that consists of two or more chemical elements, at least one of which is metal.[12] All metals have specific melting temperatures, above which they exist as amorphous liquids and below which they exist as

crystalline solids. This melting temperature is of great interest to dental laboratories, since many metallic dental structures are prepared by casting. Once cooled, a metal will form crystals; during this process the system contains both a liquid metal phase and solid crystalline grains. The crystallization is controlled by the diffusion of atoms in the molten metal to the developing solid nuclei. The crystals form and grow separately throughout the liquid phase until the entire system solidifies. The crystals solidify in random orientations and the size of the crystals will depend on the length of time they were allowed to grow before they were solidifying in place. Thus, the microscopic structure consists of crystals of different sizes randomly oriented throughout the metallic mass.[12]

Any homogenous, physically distinct, and mechanically separable portion of the microstructure is known as an alloy phase. The phases in a solid state metal solution separate out into tiny grains which are evenly distributed throughout the alloy. In solid solutions, the atoms of the two (or more) metals are located in the same crystals. Seven crystal systems are possible including cubic, tetragonal, orthorhombic, monoclinic, triclinic, hexagonal, and rhombohedral. The crystal systems are defined by the angle between the three primary axes (x, y, z) in three dimensions and the relative length of the axes. Variations of each crystal system exist to form the 14 space lattices (simple cubic, body-centered cubic (bcc), face-centered cubic (fcc), simple tetragonal, body-centered tetragonal, simple orthorhombic, body-centered orthorhombic, base-centered orthorhombic, face-centered orthorhombic, simple rhombohedral, simple hexagonal, simple monoclinic, base-centered monoclinic, and simple triclinic). In metallurgy, equilibrium phase diagrams are of great importance because they display the phases present of a given alloy system for different compositions and temperatures. They

typically exist as binary phase diagrams where the phases present for two alloying elements are considered. Ternary phase diagrams also sometimes exist and contain phase relations in a three-dimensional triangle with each element a corner of the triangle.

Each individual grain that forms consists of a single crystal. Their size depends upon the speed of cooling with rapid cooling resulting in finer grains. The longer it takes for an alloy to cool down, the more time the grains have to grow, and the larger they will become. So, a smaller grain size is achieved by rapid cooling of the molten metal. The size of grains affects properties with smaller grains producing a relatively stronger alloy with more composition uniformity resulting in increase corrosion resistance. Composition may also affect grain structure. Formation of small, equiaxed grains may be accomplished by adding tiny amounts of a very high melting metal such as iridium, rhenium, or ruthenium. These are called "grain refiners" and they solidify very early in the cooling process. They then act as nuclei around which the grains can form, resulting in smaller relative grains of approximate equal dimension.[12]

Without grain refiners, the pattern of crystallization often resembles the branches of a tree, yielding elongated crystals that are called dendrites. In alloys, the dendrites form due to a process called constitutional supercooling whereas for pure metals they form by thermal supercooling. In dentistry, most high noble and noble alloys solidify with an equiaxed microstructure, while dendritic microstructures are frequently observed in base metal casting alloys.[12]

**Equipment used to observe microstructure and characterize alloys**

Optical microscopy and scanning electron microscopy (SEM) are the most important analytical tools for studying the microstructure of alloys and will be discussed in broad terms below.

Optical microscopes utilize reflected light to examine metals. They may be classified as upright or inverted, depending on the orientation of the plane of the specimen during the observation. The optical microscope can be used to examine as-polished or etched metallographic specimens, where the purpose of etching is to reveal the grain structure and/or phases present. Its main advantage is that at low magnification optical microscopy is superior to other methods for viewing relatively flat specimens. However, the light optical microscope has a severe limitation in terms of depth of focus which restricts its use for fractographic and other failure analyses. Also, it has a moderate limitation in resolution for the examination of microstructures.1[3] Additionally, identification of unknown constituents may be aided by observation of their hardness, natural color, response to polarized light, and by the response to selective etchants.[13]

Scanning electron microscopy is one of the most versatile techniques for investigating the microstructure of metallic materials.[14] In SEM, an electron beam is focused onto a sample and an image is built from the interaction of that beam with the material. If the incoming electrons are elastically scattered, they are known as backscattered electrons. Alternatively, the incoming electrons may scatter loosely bound electrons from the surface atoms, resulting in what are termed secondary electrons. For either backscattered or secondary electrons, a detector synchronized with the scanning beam will detect their intensity and convert it to an image. SEM advantages are that it is

able to view specimens at increased magnification compared to the optical microscope. Due to its better depth of field compared to a light microscope, it is also useful for the magnification of fracture surfaces and deeply etched metals. Specifically, its magnification may reach up to 50,000X and its depth of field is 300 times that of an optical microscope.[14]

Frequently coupled with an SEM is a composition determining technique in the form of electron probe microanalysis (EPMA). When the electron beam in SEM strikes a sample, the incoming electrons knock inner shell electrons out of the atoms in the sample as mentioned above. As outer shell electrons drop into the vacancy created, they are obliged to dispose of the excess energy, often as an x-ray photon. Since each element has its own unique set of energy levels, the emitted x-rays are indicative of the element that produced them; they are characteristic x-rays. Analyzers are used to characterize the x-rays for energy (energy dispersive spectroscopy; EDS or EDX) or wavelength (wavelength dispersive spectroscopy; WDS) and abundance to determine the composition of sample.[14] With certain EPMA systems, it is possible to map out areas of elemental concentration whereas other determine composition of points or lines. Mapped out elemental areas are useful in analyzing the segregation of certain elements in the microstructure of an alloy.

Another method useful for characterizing metals as well as other crystalline materials is x-ray diffraction (XRD). X-rays were discovered by Roentgen in 1895. In x-ray diffraction, a beam of x-rays strike a crystal or crystals and interact with the various planes of atoms in the crystal.[15] Destructive interference of the scattered x-rays takes place in all directions except those predicted by Bragg's Law, which represents

constructive interference of those waves as they are in phase. An x-ray beam is diffracted when certain geometrical conditions are met as given by Bragg's Law which is:

$$n\lambda = 2d \sin\theta$$

where n is an integer, $\lambda$ is the wavelength of the incident x-rays, d is the interplanar spacing, and $\theta$ is the angle. The angle of the incoming beam and plane of atoms has to equal the angle of the diffracted beam and plane of atoms. If the angles are not equal, the radiation is not in phase and cancels by interference. From the angles and intensities of these diffracted beams, information may be obtained depending upon technique variables. Among the possibilities include identification of a compound, determination of phases and unit cell dimensions, magnitude of strain, existence of preferred orientation, etc.[15]

**NiCr and CoCr metallurgy**

Baran[16] reviewed the metallurgical properties of NiCr alloys. The binary phase diagram shows extensive solid solubility of chromium in nickel (approximately 37 wt%). Chromium provides corrosion resistance and some solid solution hardening, while other alloying elements are used to provide more solid solution hardening or precipitation formation. Elements contributing to solid solution strengthening include aluminum, tungsten, and molybdenum. Addition of carbon, boron, silicon, and aluminum are known to stimulate precipitate formation. Boron, gallium, and beryllium are effective in lowering the melting range of the alloy. The dendritic microstructure of Ni casting alloys during solidification remains relatively immune to heat treatments encountered during dental laboratory processing. Beryllium-containing alloys have been shown to contain a NiBe phase located between dendrites of the primary solid solution. NiCr alloys possess

excellent resistance to tarnish in a sulfide medium and the corrosion resistance decreased when the chromium content was less than 16%. Microscopic examination revealed that corrosion attack occurred in chromium depleted regions.

Wylie et al.[9] observed the microstructure and corrosion behavior (electrochemical measurements) of two NiCr-based dental casting alloys in artificial saliva at different pHs in the presence of a crevice before and after heat treatment. The microstructure was studied using optical microscopy, scanning electron microscopy, and energy dispersive x-ray analysis. Disc-shaped specimens were formed following the manufacturer's instructions for casting. The microstructure characterization showed a dendritic microstructure for the two NiCr alloys after electroetching. After heat treatment, the microstructure and corrosion properties showed insignificant changes. The higher Cr-containing alloy (25 wt%) showed superior corrosion resistance than the alloy containing less Cr (12.6 wt%). Selective dissolution occurred at regions within the microstructure containing lower levels of Cr and Mo.

Since metal-ceramic processing steps of oxidation and porcelain baking are basically forms of heat treatment, alloy phase changes may occur that affects its stability when used for such devices. Along this line, Baran[11] investigated five commercial, NiCr alloys after heat treatment and porcelain baking. Different types of etchants were used. It was found for four of the five alloys that depletion of alloying elements from the matrix due to their outward diffusion occurred during oxidation treatments (but not porcelain baking).

The oxidation of dental casting alloys occurs as a preliminary step and during porcelain fusing at elevated temperature. Baran[10] in 1983 measured the oxidation kinetics

of NiCr dental alloys using a commercial thermal analysis system as a function of composition, temperature, alloy microstructure, and dental laboratory procedure. He found that the kinetics of oxidation were more strongly influenced by the temperature than the oxygen partial pressure. The different alloys behaved differently in terms of the amount of weight gain (reflective of oxidation) squared versus time, some exhibiting a parabolic relationship at high temperature whereas others followed a linear pattern at lower temperatures. It was also observed that high-purity nickel oxidizes more rapidly than the NiCr alloys.

Baran[17] chemically analyzed four commercially available NiCr alloys with a scanning Auger microprobe. Baran determined the composition of oxide layers on selected NiCr porcelain-fused-to-metal (PFM) alloys in three temperature domains and in two different atmospheres, as well as the distribution patterns of elements in the oxide. Distributions of Ni and Cr in the oxide layers varied with the alloy and oxidation in air resulted in thicker oxide layers than did oxidation in a reduced oxygen atmosphere. It was also observed that the chromium content alone does not determine the nature of the Cr distribution pattern in the oxide.

Baran[18] investigated and identified the compounds formed on NiCr alloys during oxidation procedures similar to those encountered during alloy processing used for metal-ceramic systems. X-ray diffraction was used to analyze the compounds formed on five NiCr alloys after oxidation. Oxides of nearly all elements contained in the alloys were found after low temperature (650°C) oxidation, while NiO and particularly $Cr_2O_3$ were predominant after oxidation at high temperatures (1000°C).

Lin et al.[19] evaluated the effects of a PFM firing process on the microstructure, surface oxide composition, and corrosion behavior of two commercial NiCr alloys. Two types of alloy were tested: a high Cr and Mo Ni-based alloy without Be and a low Cr and Mo Ni-based alloy with Be. After firing, the microstructure showed new interdendritic precipitates. Also, there was a slight increase in $CrO_2$ on the surface of the Be-free alloy and increased amounts of Mo and Ni were observed on the surface of both alloys. Despite these surface changes, the corrosion properties of the alloys were not significantly different after firing compared to before firing.

Huang[6] investigated the influence of composition on the corrosion behavior of NiCrMo dental casting alloys in an acidic artificial saliva. Corrosion resistance of the NiCrMo casting alloys is associated with the formation of a passive film containing $Ni(OH)_2$, NiO, $Cr_2O_3$, and $MoO_3$ on the surface. The NiCrMo alloys with higher Cr and Mo contents had a much larger passive range on their polarization curves and were immune to pitting corrosion due to the presence of high amounts of Cr (maximum ~31–35%) and Mo (maximum ~12%) contents in the surface passive film.

Huget et al.[20] investigated the composition, microstructure, mechanical properties, and alloy-porcelain bond strength of two NiCr-based crown and bridge alloys, Wiron-S and Microbond-NP. Despite only slight composition differences between the alloys primarily with less abundant alloying elements, Wiron-S was significantly stronger than Microbond-NP. The authors believed this was due to microstructural features and noted the Microbond-NP alloy appeared to be more homogenized after porcelain firing. Microbond-NP yielded alloy-porcelain bond strength values comparable to those of noble

alloy-porcelain combinations, whereas Wiron-S needed a coating agent to bond sufficiently to porcelain.

Roach et al.[21] evaluated the changes in alloy surface oxides and electrochemical corrosion properties of 6 NiCr alloys after PFM firing. Results indicated an increase in corrosion rates after PFM firing and repolishing. This increase in corrosion rate was attributed to a decrease in the Cr and Mo content in the surface oxide layer. The PFM firing and repolishing process did not alter the corrosion behavior of the alloys containing lower levels of Cr and Mo. Si particles became embedded in the surfaces of the fired alloys during repolishing and may have contributed to the changes in surface oxides and the corrosion behavior of some alloys.

Asgar and Allan[22] studied the microstructure of four CoCr alloy types that are used for partial denture castings. Type I are the most basic alloys, have been used in dentistry for many years, and contain 60% Co and 25% Cr. The microstructure of Type I alloy showed that the grains are large and large carbides also form. The presence of these massive carbides lowers the ductility of the alloys. Casting at higher temperatures, however, results in the dispersion of the carbides. In Type II alloys, the effects of the less traditional CoCr alloying additions (Ga, Zr, Cu, etc.) were demonstrated. The addition of gallium decreased the grain size because gallium has a low melting point. The addition of zirconium and boron raised the melting temperature of the alloy, which caused carbides to be dispersed and distributed within the grain rather than precipitated at the grain boundaries.

Reclaru et al.[23] compared the corrosion behavior of noble metal (Au, Pt, Ru) containing CoCr-based alloys with conventional CoCr based alloys. Their

microstructures were analyzed before and after electrochemical corrosion tests. The corrosion resistance of the CoCr alloys was significantly reduced with the additions of the noble metals. The additions of Au, Pt, and Ru resulted in a heterogeneous microstructure with spherical precipitates that seemed to be responsible for the reduction in corrosion resistance.

In a more detailed account of the above study, Reclaru et al.[24] again measured corrosion resistance and characterized the microstructure of CoCr doped with Au, Pt, and Ru. The results again showed that the presence of the noble metals deteriorated the corrosion resistance of the CoCr alloys in a significant way. In terms of microstructure, gold doping produced a heterogeneous microstructure that was vulnerable to corrosive attack.

**Metallurgy of palladium-based alloys**

Vermilyea et al.[25] investigated the metallurgical structure of high-palladium alloys for metal-ceramic restorations. Three alloys containing at least 75 wt% palladium and one alloy containing less palladium (60 wt%) but increased silver (28 wt%) were studied. Ten castings of each alloy designed to simulate a maxillary central incisor coping were used for investigation of as-cast and heat-treated (simulated porcelain firing) conditions. All specimens were metallographically polished and etched with aqua regia. The microstructure analysis of as-cast and heat treated specimens was done by SEM. SEM images of as-cast alloys showed an equiaxed fine-grain structure with considerable microsegregation but after heat treatment, homogenization of the microstructures occurred.

Brantley et al.[26] used x-ray diffraction to investigate the metallurgical phases of four as-cast high-palladium alloys. Two PdCuGa alloys and two PdGa alloys were cast into plate-shaped specimens and analyzed using two different x-ray diffractometers. All four alloys exhibited strong XRD peaks for the face-centered cubic (fcc) palladium solid solution matrix and the alloys displayed a preferred crystallographic orientation. PdCuGa alloys contained appreciable amounts of near-surface lamellar interdendritic or eutectic constituents. PdGa alloys contained low-intensity peaks which attributed to small amounts of secondary phases observed in the microstructures.

In a follow-up study, Brantley et al.[27] investigated the metallurgical phases of four oxidized high-palladium alloys (two PdCuGa alloys and two PdGa alloys) by x-ray diffraction. The surface preparation procedure had a profound effect on the phases present in the oxide layers. The oxide layers on both PdCuGa alloys contained $Cu_2O$ and $\beta$-$Ga_2O_3$. The principal phase in the oxide layers of both PdGa alloys was $In_2O_3$, which exhibited extreme preferred orientation. For the air-abraded specimens, $\beta$-$Ga_2O_3$, was not present in the oxide layers on the PdCuGa alloys, and $\beta$-$Ga_2O_3$ was the major phase in the oxide layers on the PdGa alloys.

**Past relevant studies**

Being newly introduced to the market, very little peer-reviewed literature is available on the CoPdCr and NiPdCr alloys apart from the following two reports evaluating the electrochemical properties of the alloys.

Sarantopoulos et al.[4] compared the corrosion properties of traditional CoCr and NiCr casting alloys with the palladium-containing CoCr and NiCr counterparts.

Specifically, the casting alloys investigated were: 1 palladium-containing nickel-chromium alloy (NiPdCr: NobleCrown from the Argen Corporation), two palladium-containing cobalt-chromium alloys (CoPdCr-A: Noble Crown NF from Argen and CoPdCr-I: Calisto CP+ from Ivoclar Vivadent, Inc.) and traditional NiCr (Argeloy N.P. Star from Argen) and CoCr (Argeloy N.P. Special from Argen) alloys. As-cast and oxidized cylindrical specimens were evaluated electrochemically in phosphate buffered saline using a computer driven potentiostat. The electrochemical data collected consisted of monitoring the open circuit potential (OCP) for 20 hrs followed by conducting linear polarization and cyclic polarization tests. Light microscopy was used to examine the alloy surfaces before and after electrochemical testing. The authors found that the addition of palladium significantly increased the OCP, but the corrosion current density was significantly greater and the polarization resistance was less compared to the traditional alloys without palladium. Also, a greater incidence of pitting was observed in the palladium-containing alloys.

Beck et al.[5] evaluated the elemental release of the same CoPdCr, NiPdCr, CoCr, and NiCr alloys. The CoPdCr alloys released a significantly greater amount of respective ions (Co, Cr, Mo, and total ions) compared to the traditional CoCr alloy. No significant differences in elemental release were noted between NiPdCr and NiCr. Consistent with the Sarantopoulos et al. study, corrosion resistance was compromised when CoCr was alloyed with palladium. However, this effect was not observed with NiCr.

# MATERIALS AND METHODS

Two palladium-containing CoCr alloys (NobleCrown NF and Callisto CP+) and 1 palladium-containing NiCr alloy (Noble Crown) were evaluated and compared to traditional CoCr and NiCr alloy (Argeloy N.P. Special and Argeloy N.P. Star, respectively). The compositions of these 5 alloys with their manufacturers are listed in Table 1. The alloys were cast into a cylindrical shape using a sectioned plastic rod as a casting pattern (14 mm height × 4.8 mm diameter; n=10). The plastic rod sections were sprued, invested in a carbon-free, phosphate bonded investment (Formula 1; Whip Mix Corp, Louisville, KY), and burned out. Casting was performed by a private dental laboratory (Capitol Dental Lab, Menomonee Falls, WI) following manufacturer instructions using individual quartz crucibles (Type S-Slotted; Select Dental Manufacturing, Farmingdale, NY) for each alloy, a multiorifice gas-oxygen torch, and centrifugal casting machine.

Table 1. Elemental compositions (wt%) of the alloys provided by the manufacturers

| Alloy Name | Code | Manufacturer | Composition (wt%) | | | | | |
|---|---|---|---|---|---|---|---|---|
| | | | Co | Ni | Pd | Cr | Mo | Other |
| NobleCrown NF | CoPdCr-A | The Argen Corporation (San Diego, CA) | 45 | - | 25 | 20 | 10 | B |
| Callisto CP+ | CoPdCr-I | Ivoclar Vivadent, Inc. (Amherst, NY) | 40 | - | 25 | 21.4 | 12.7 | <1 W, B, Ta |
| Argeloy N.P. Special | CoCr | Argen | 59.5 | - | - | 31.5 | 5 | 2.0 Si; 1.0 Mn; 1.0 Other |
| Argeloy N.P. Star | NiCr | Argen | - | 61.2 | - | 25.8 | 11 | Al; Mn; 1.5 Si |
| Noble Crown | NiPdCr | Argen | - | 37.5 | 25 | 25 | 12 | Si |

Divested specimens were mounted in epoxy resin (Sampl-Kwick, Buehler, Lake Bluff, IL). All specimens were ground following standard metallographic procedures

with 1200 grit silicon carbide paper (Carbimet Discs; Buehler) used for final grinding. Finally, all specimens were polished with a 1.0 and 0.3 μm alumina suspension (Alpha Micropolish Alumina, Buehler).

**Optical microscopy**

For viewing the microstructure, the NiCr and Co-containing alloys were etched in a solution of nitric acid and concentrated hydrochloric acid in a molar ratio of 1:3. The NiPdCr alloy was etched in a mixture of 80 vol% hydrochloric acid and 20 vol% hydrogen peroxide. The alloys were etched for progressive time intervals until the microstructure was revealed. A metallurgical microscope (Olympus PME3, LECO Corporation, St. Joseph, MI) with a digital image acquisition device (SPOT Insight 2MP Firewire Mono, Diagnostic Instruments Inc., Sterling Heights, MI) and software (SPOT Software 4.5, Diagnostic Instruments Inc.) was used to evaluate the specimens and obtain digital micrographs. Magnifications of 50x, 100x, 200x, and 500x were used for obtaining micrographs.

**Scanning electron microscopy/electron probe microanalysis**

Scanning electron microscopy (X-650, Hitachi, Tokyo, Japan) with electron probe microanalysis was used to evaluate the microstructure of alloys with regard to composition. EPMA was conducted on the area shown on the SEM image obtained using a backscattered electron detector. Instrument and scan parameters consisted of: an electron acceleration voltage of 15 kV, a beam size of 1 μm, and a step size of 1 μm in the x and y directions scanning an area of 240×240 μm. For the given image, elemental

maps corresponding to Co or Ni, Pd, Cr, and Mo were collected using EPMA. The EPMA images were color coded to correspond to relative concentration of the respective element.

**X-ray diffraction**

The alloys were analyzed with a micro-XRD unit (RINT-2500, Rigaku Corporation, Tokyo, Japan) using Cu Kα radiation (λ=1.54 Å) with an excitation voltage of 50 kV and tube current of 300 mA with a Ni filter. Scans were conducted over a 2θ range of 20 to 140$^{o}$ using a step size of 0.05$^{o}$. XRD pattern peaks were compared to pure metals using ICDD-2000 files (International Center for Diffraction Data, Swarthmore, PA). The XRD pattern of the resin used to mount the specimens was also acquired to separate out any peaks arising from the mounting material. The XRD spectra peaks were indexed to determine planes and lattice parameters following procedures described by Cullity.[15]

**Vickers microhardness**

Separate as-cast cylindrical alloy specimens (n=4/alloy) not analyzed with the above procedures were mounted in epoxy resin and prepared with standard metallographic procedures, i.e. grinding with successive grades of SiC paper and polishing with a 1 μm alumina suspension. The microhardness of the alloys was tested with a Vickers microhardness tester (Kentron; Torsion Balance Co., Clifton, NJ) using a 500 g load and dwell time of 15 seconds. Each alloy specimen was indented twice, with the average of each indent then averaged among the four specimens per alloy. The

Vickers microhardness number (VHN) was calculated according to the following formula:

$$VHN = 2 * F * \sin(136^{o}/2) / d^{2}$$

Where F is the applied load in kgf and d is the average length of the indent diagonals in mm. The $136^{o}$ accounts for the angle between the faces of the diamond pyramid indenter.

**Statistical analysis**

Vickers microhardness was statistically analyzed by one way ANOVA and Tukey's HSD test ($\alpha$=0.05) using SPSS statistical software (version 17.0; SPSS, Inc. Chicago, IL).

# RESULTS

## Optical microscopy

The optical microscopy results are shown in Figures 1-15. For each alloy, a representative image of the microstructure is presented for magnifications of 50x, 100x, and 200x. The microstructure for all five alloys is characterized as dendritic in nature. Comparing the Pd-containing alloys to those of the traditional CoCr and NiCr alloys, it appears the addition of palladium resulted in microstructures of increased complexity as evidenced by the possible greater number of precipitates, secondary structures, and etching effects.

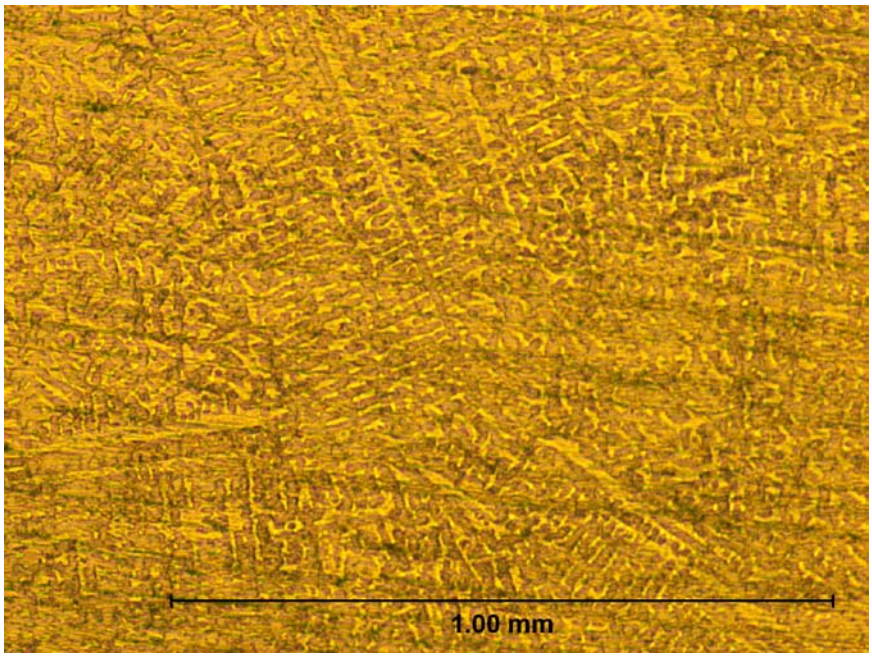


Figure 1. Optical micrograph of NiCr (50x) after etching

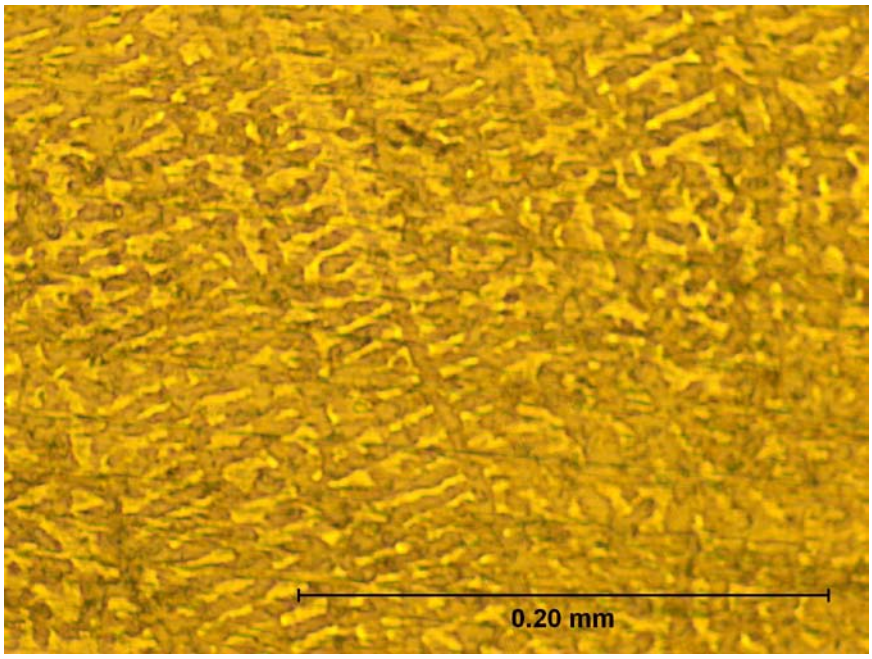


Figure 2. Optical micrograph of NiCr (100x) after etching

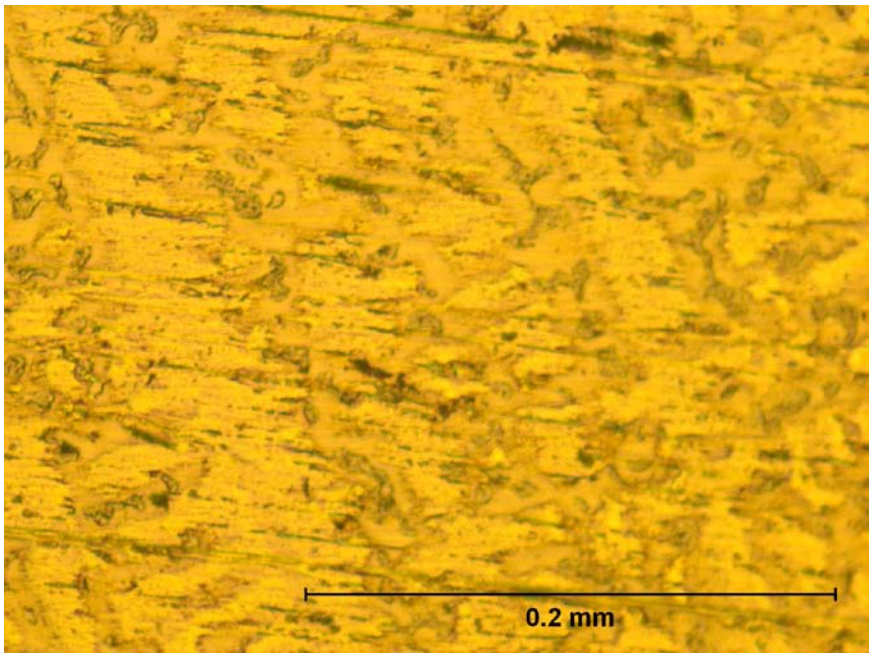


Figure 3. Optical micrograph of NiCr (200x) after etching

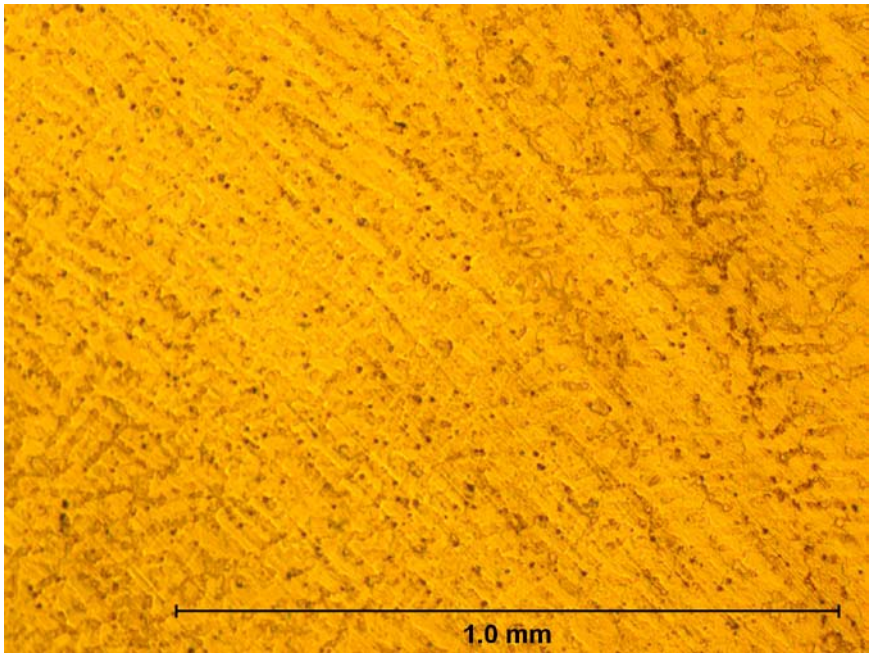


Figure 4. Optical micrograph of NiPdCr (50x) after etching

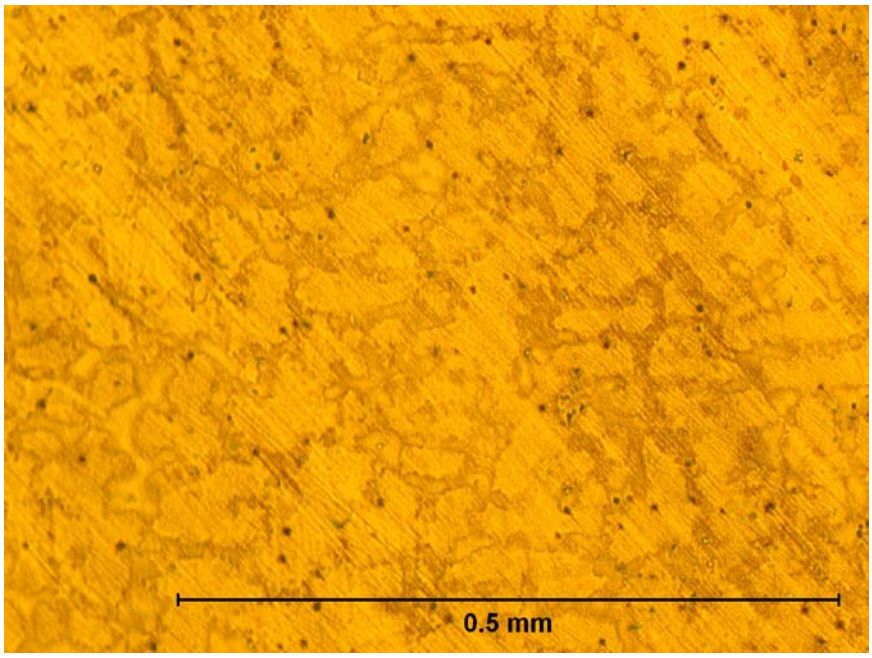


Figure 5. Optical micrograph of NiPdCr (100x) after etching

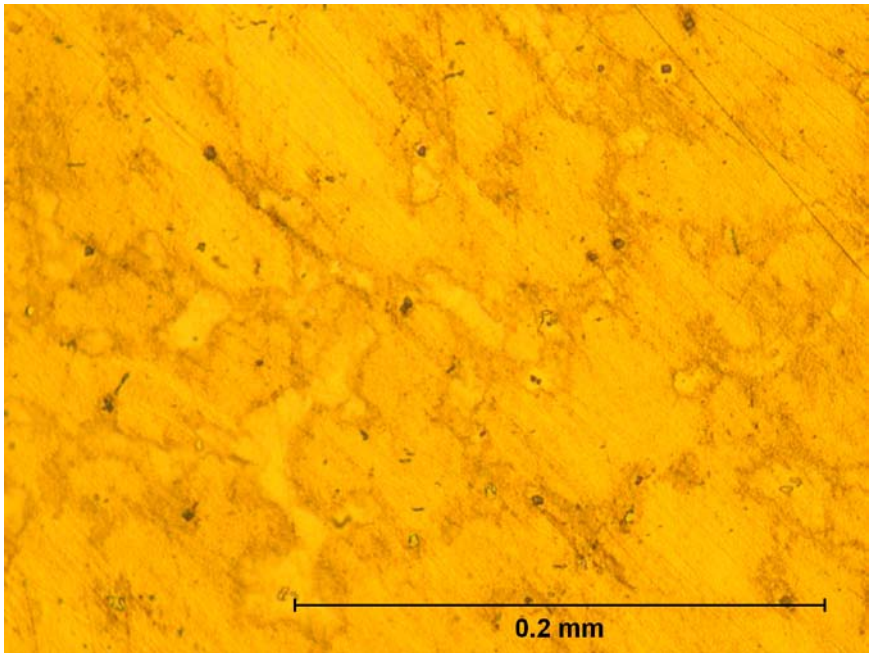


Figure 6. Optical micrograph of NiPdCr (200x) after etching

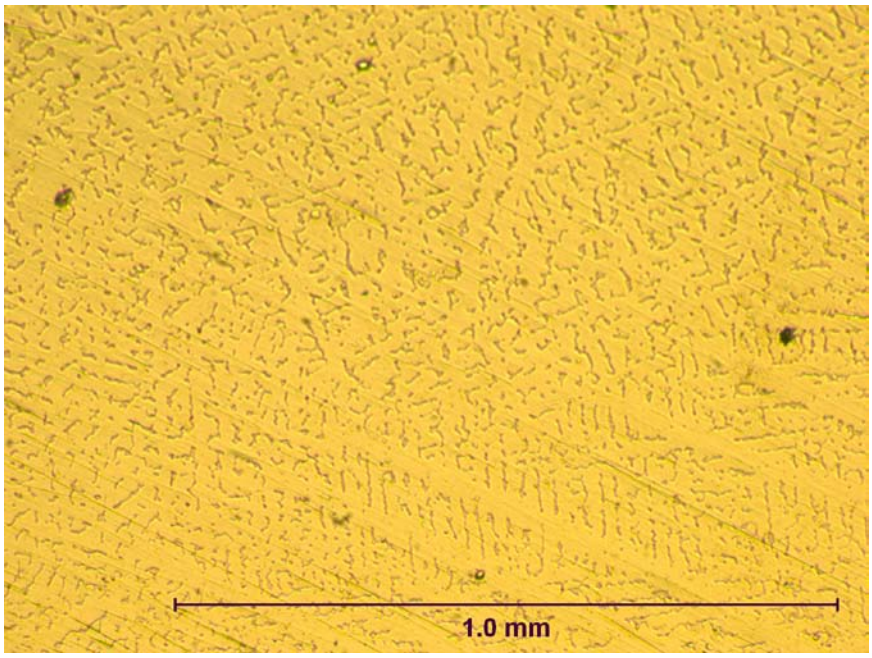


Figure 7. Optical micrograph of CoCr (50x) after etching

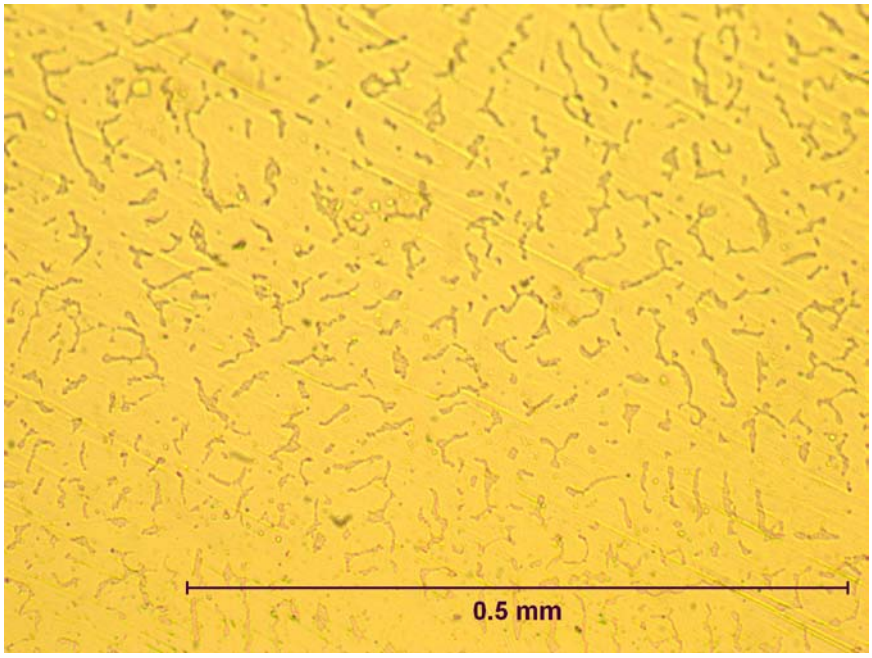


Figure 8. Optical micrograph of CoCr (100x) after etching

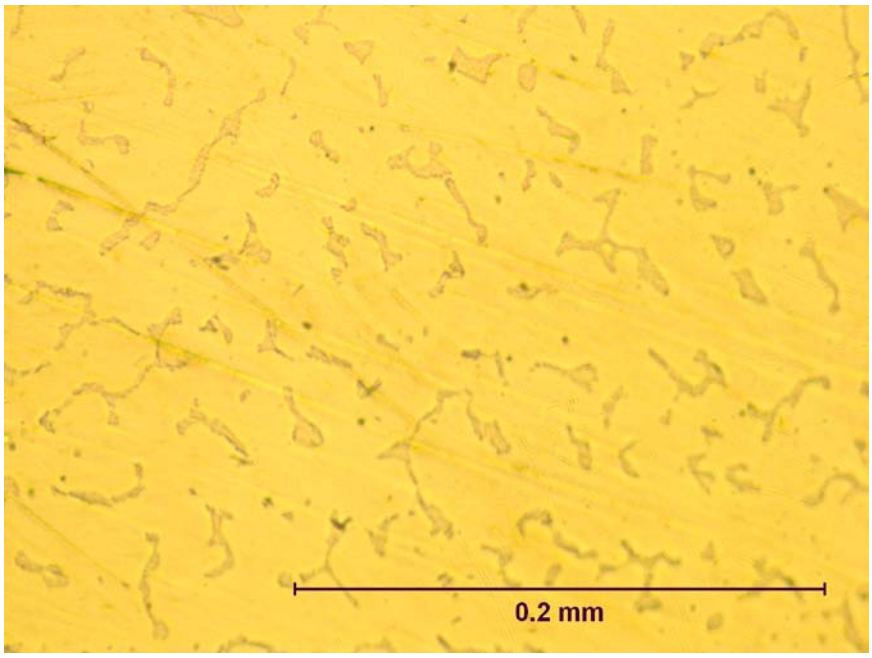


Figure 9. Optical micrograph of CoCr (200x) after etching

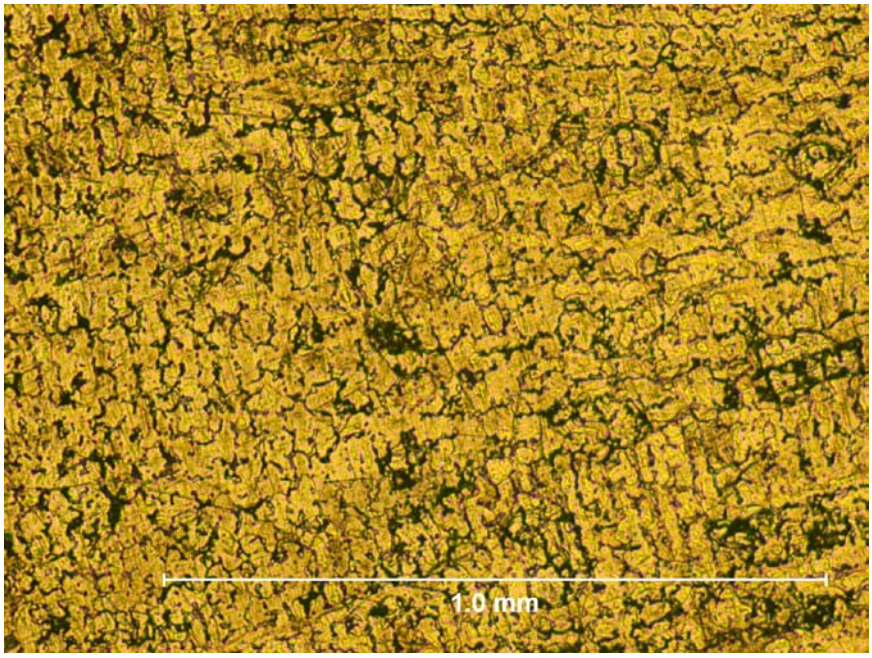


Figure 10. Optical micrograph of CoPdCr-I (50x) after etching

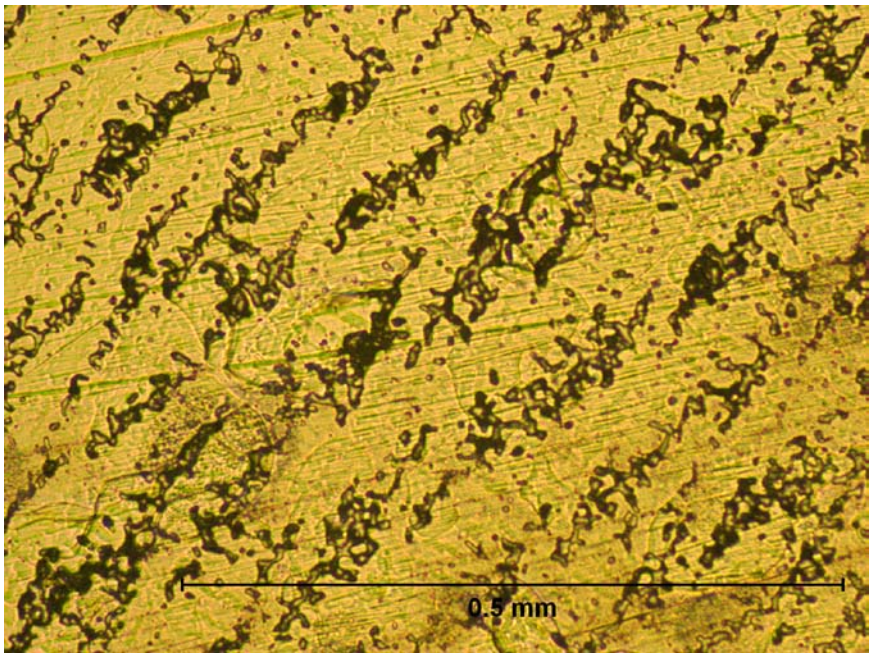


Figure 11. Optical micrograph of CoPdCr-I (100x) after etching

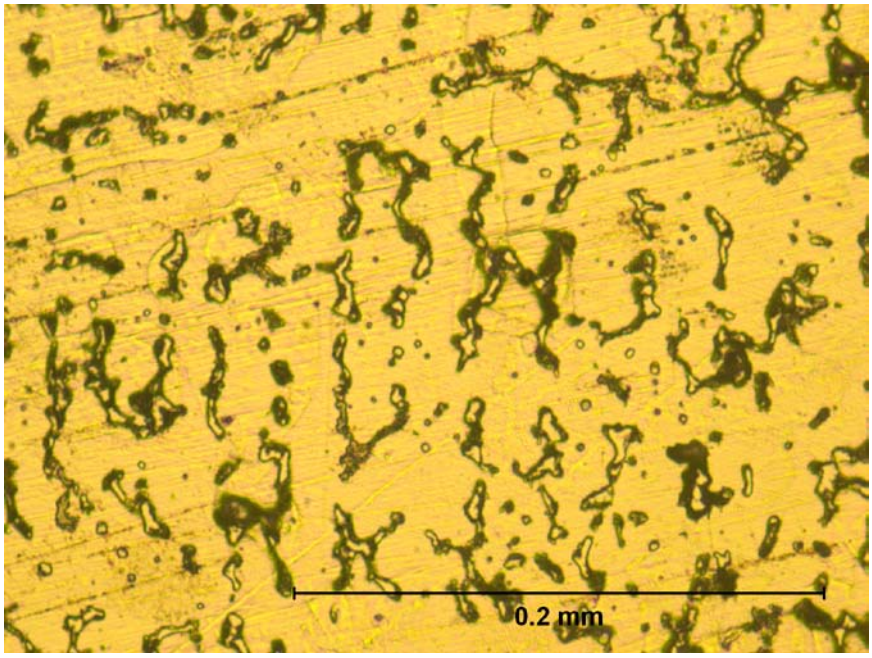


Figure 12. Optical micrograph of CoPdCr-I (200x) after etching

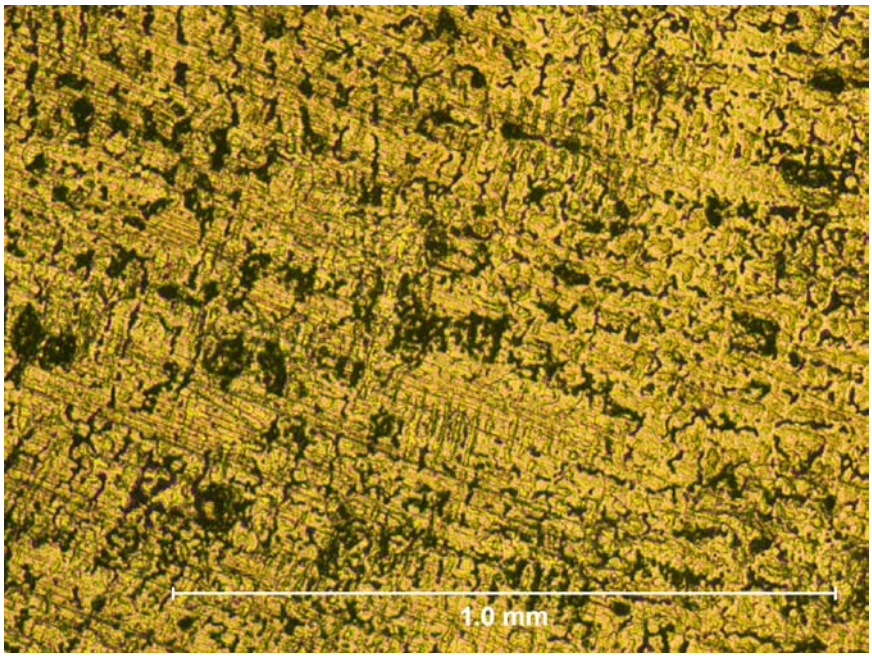


Figure 13. Optical micrograph of CoPdCr-A (50x) after etching

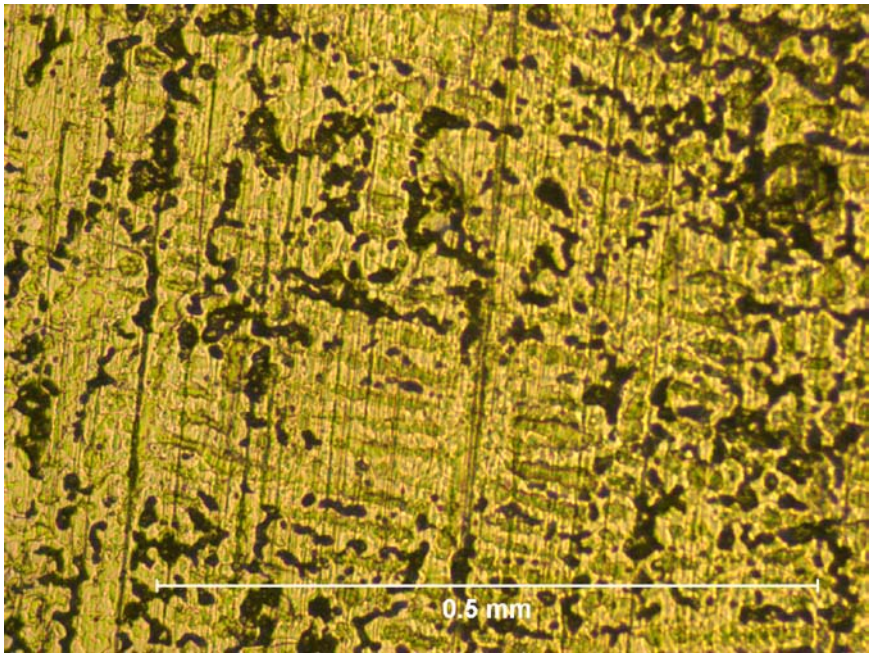


Figure 14. Optical micrograph of CoPdCr-A (100x) after etching

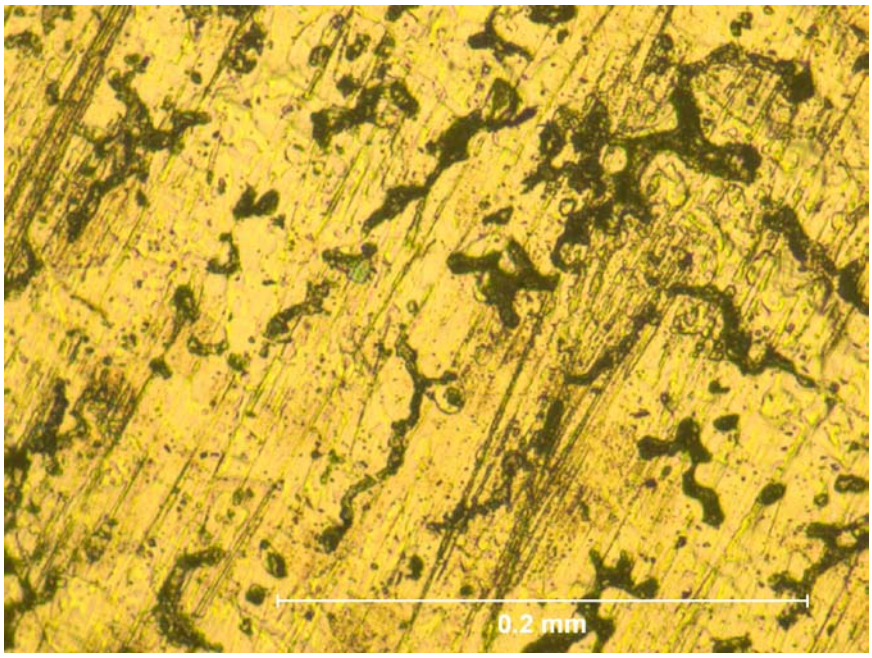


Figure 15. Optical micrograph of CoPdCr-A (200x) after etching

**Scanning electron microscopy/electron probe microanalysis**

Figures 16 and 17 show the backscattered electron images of NiPdCr and CoPdCr-A, respectively. Similar to above, a dendritic type of structure is observed. In a backscattered electron image, the brightness in the micrograph is proportional to atomic number with higher atomic number atoms showing as lighter areas. The elemental maps show chromium is relatively uniformly distributed in the microstructure as opposed to Co or Ni, Pd, and Mo where microsegregation is obvious with areas richer in Pd countering areas richer in Co or Ni and Mo.

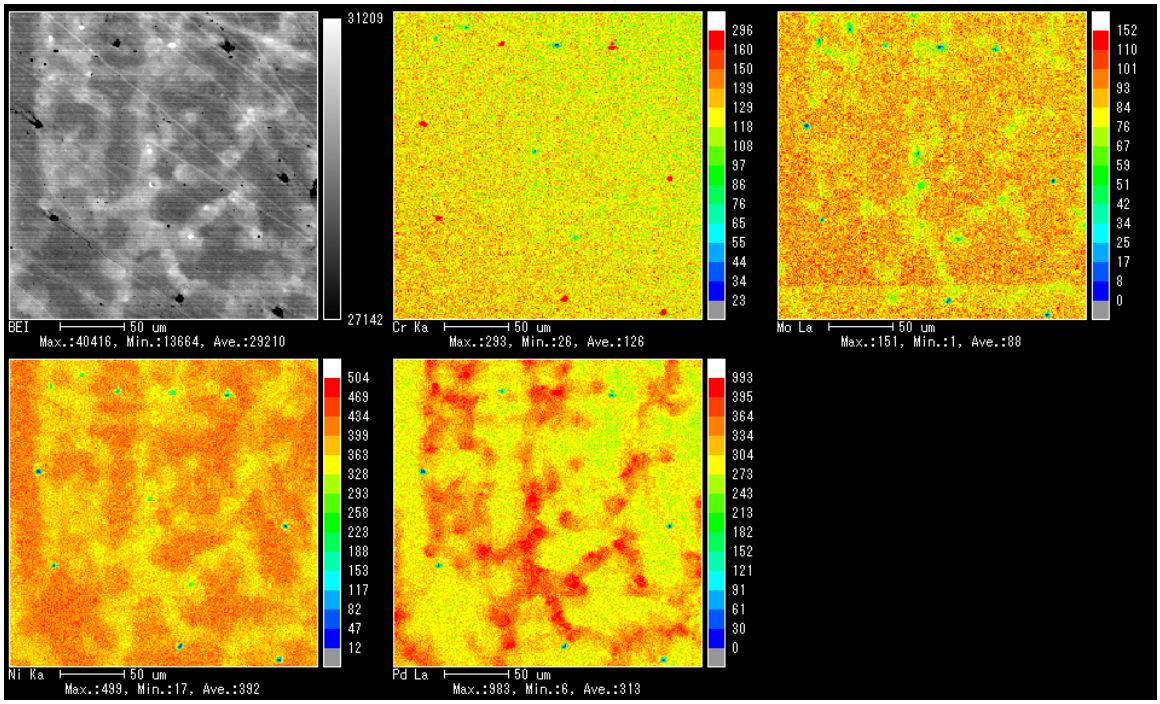


Figure 16. SEM/EPMA micrograph of NiPdCr

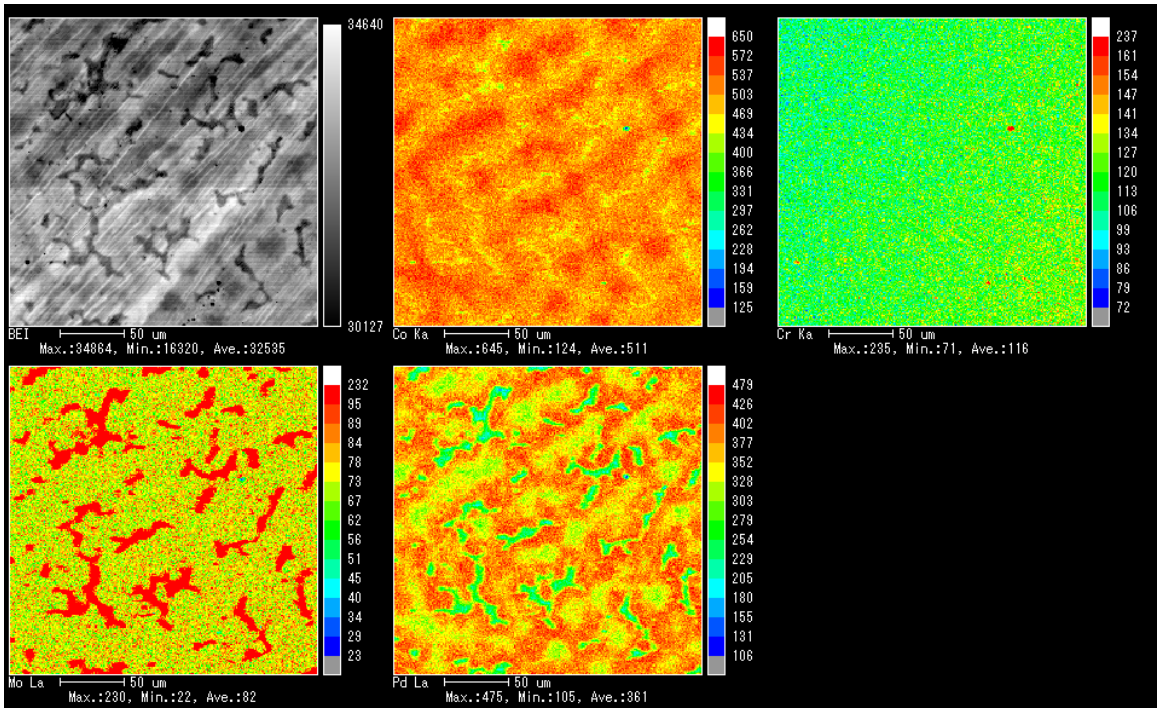


Figure 17. SEM/EPMA micrograph of CoPdCr-A

**X-ray diffraction**

The x-ray diffraction patterns for the five alloys and the resin surrounding the alloys are presented in Figures 18-23. The XRD of resin is included to allow for discrimination of any peaks arising from the resin material. For each alloy, the ICDD patterns for the major alloying elements are also included for comparison. Indexing of the XRD patterns showed the NiCr and NiPdCr alloys were primarily face centered cubic Ni solid solution. The peaks at 2θ angles of approximately 42, 50, 73, 89, and 118 degrees (if present in the given pattern below) were attributed to (111), (200), (220), (311), and (222) planes, respectively. The lattice parameters for NiCr and NiPdCr were 0.360 nm and 0.369 nm, respectively. For the Co-based alloys, slightly different spectra were obtained when comparing the CoCr to CoPdCr alloys although they would both be considered primarily Co solid solutions. The CoCr alloy best matched the ICDD pattern for hexagonal Co, whereas the CoPdCr alloys best matched the ICDD pattern for face centered cubic Co. For the CoCr alloy, the peaks at 2θ angles of approximately 41, 44, 46, 75, 83, and 91 degrees were believed to be (100), (002), (101), (110), (103), and (112) planes, respectively. For the CoPdCr alloys, the peaks at 2θ angles of approximately 21, 24, 36, 44, and 47 degrees (if present in the given pattern below) were attributed to (111), (200), (220), (311), and (222) planes, respectively. The lattice parameters for CoPdCr-A and CoPdCr-I were 0.367 nm and 0.369 nm, respectively. Comparison to the ICDD patterns suggests preferred orientation is observed in all of the alloys.

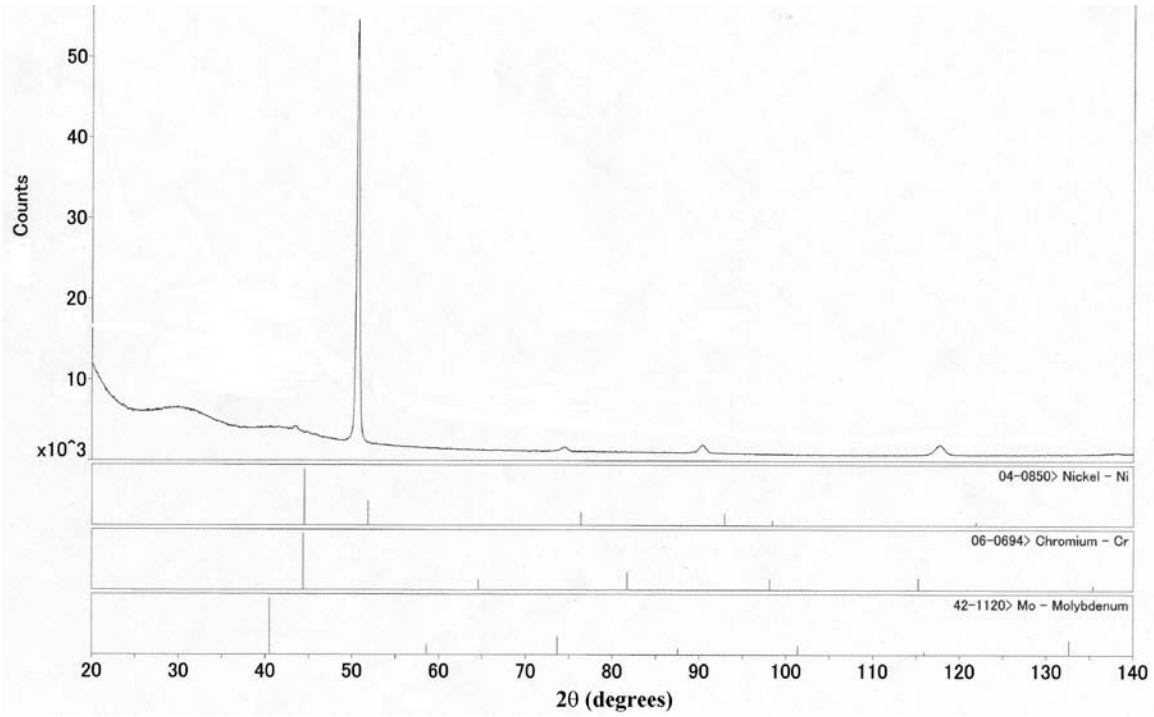


Figure 18. XRD pattern for NiCr

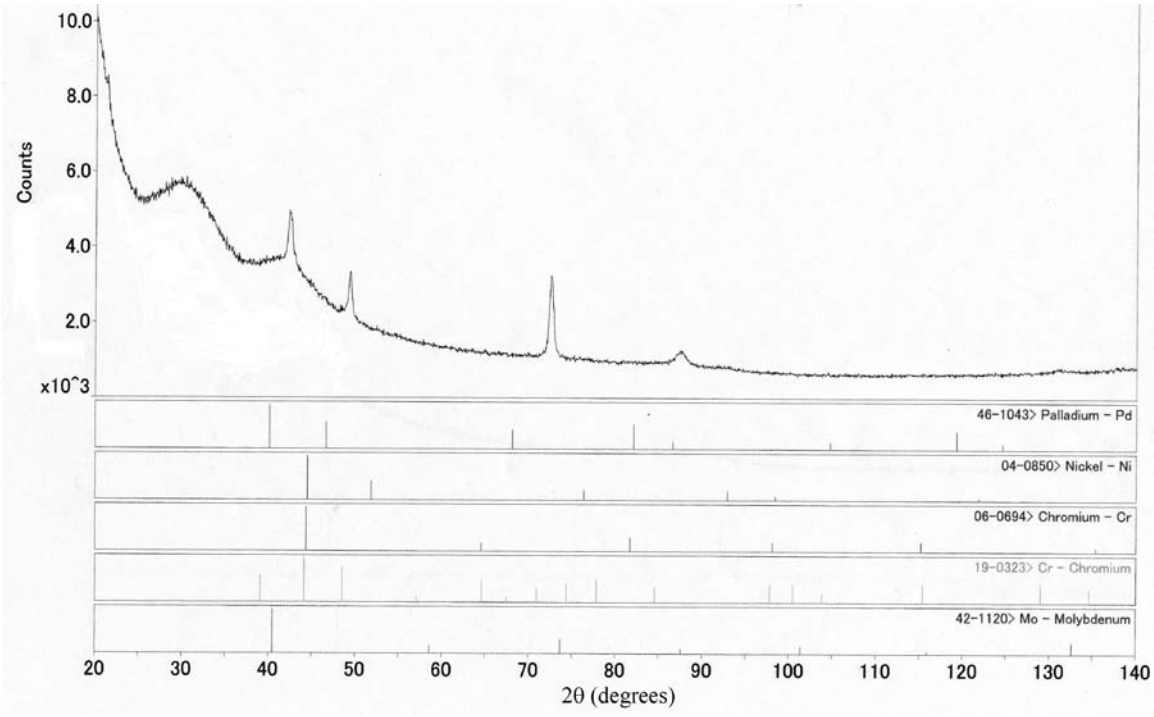


Figure 19. XRD pattern for NiPdCr

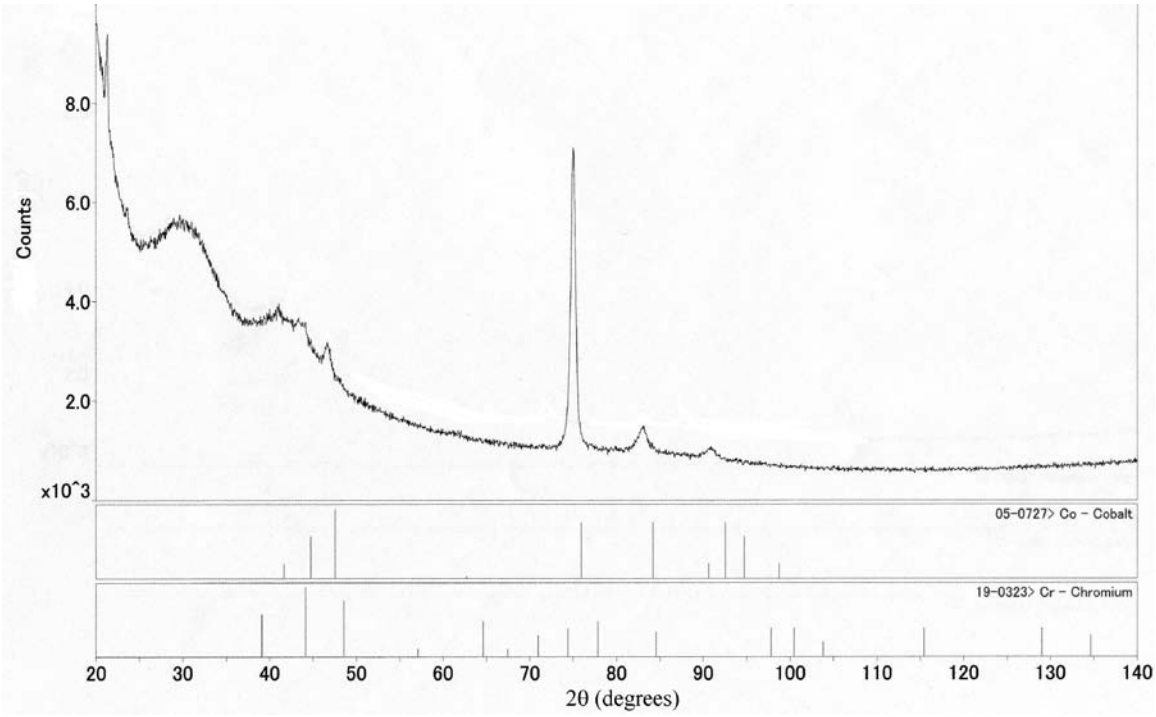


Figure 20. XRD pattern for CoCr

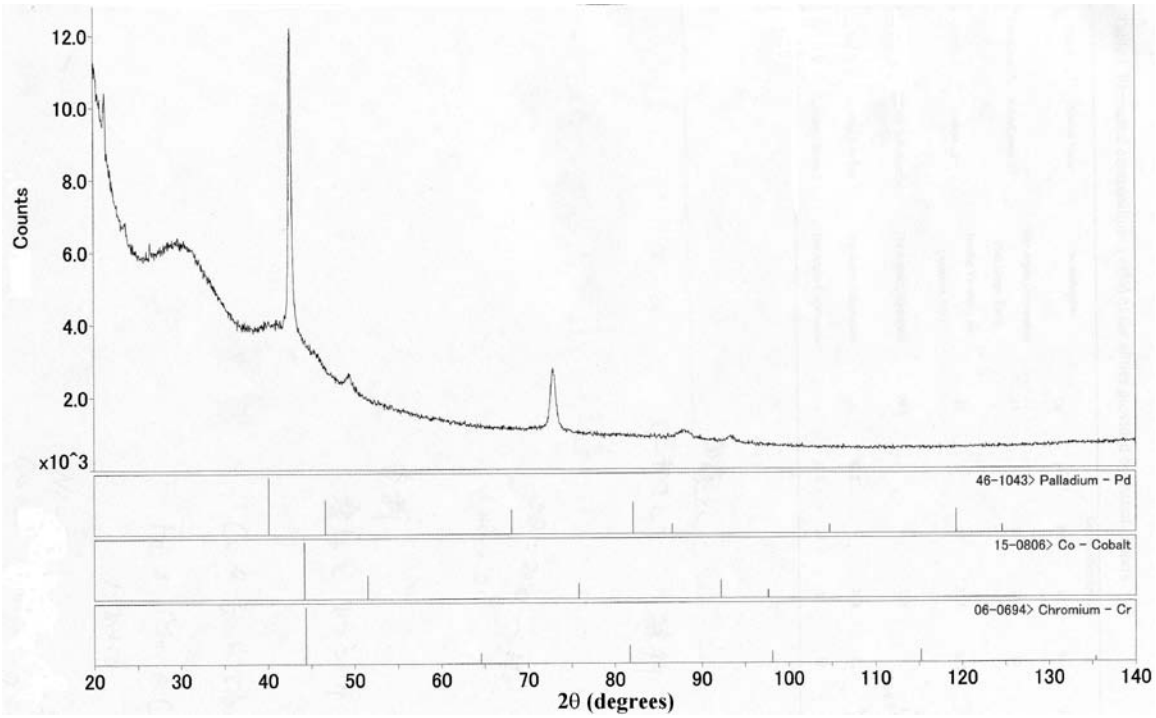


Figure 21. XRD pattern for CoPdCr-A

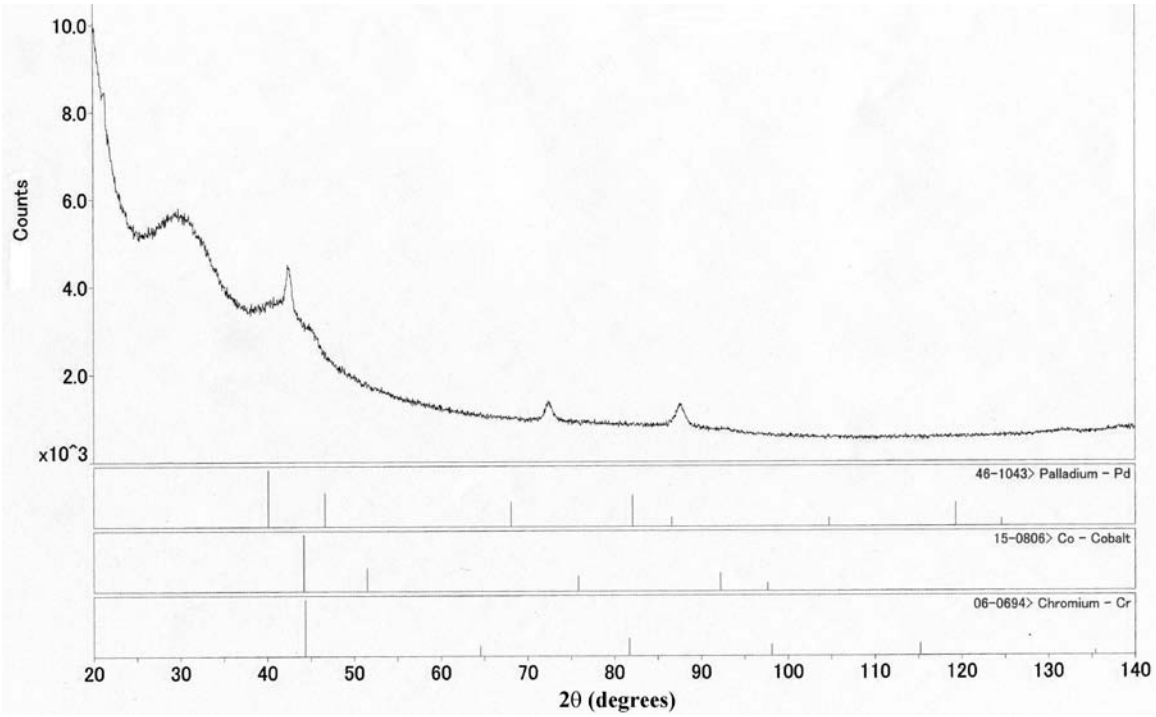


Figure 22. XRD pattern for CoPdCr-I

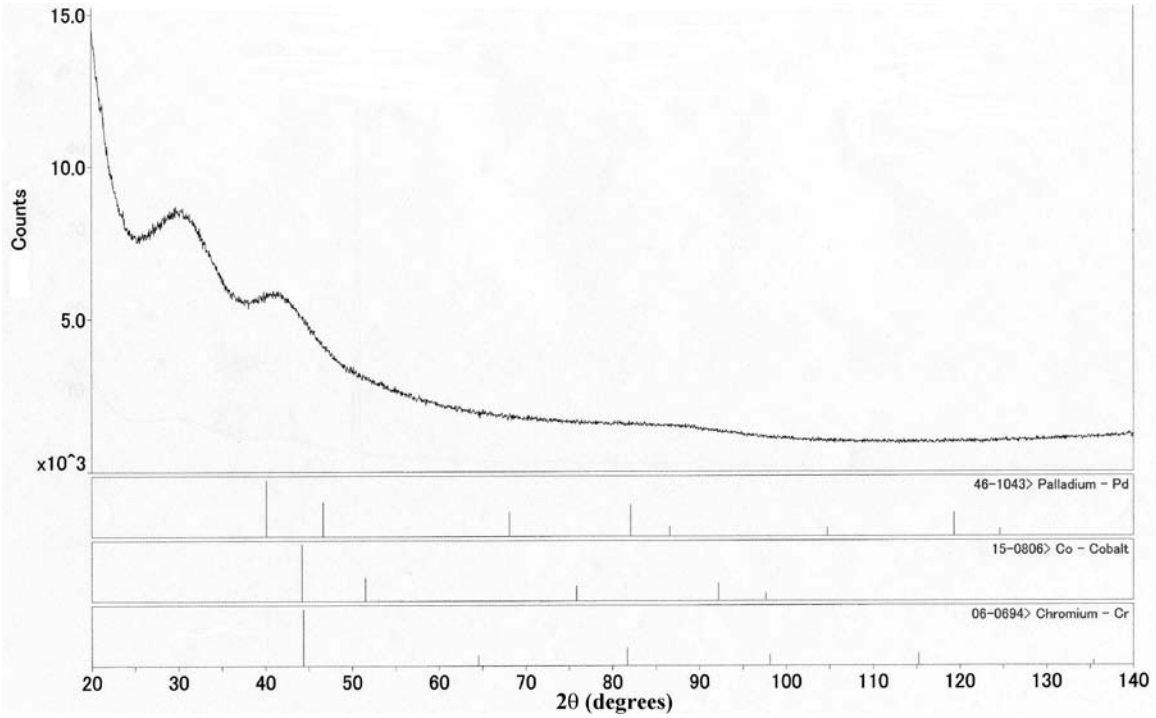


Figure 23. XRD pattern for the resin surrounding the alloys

**Vickers microhardness**

For each alloy tested, the Vickers microhardness mean values along with the standards deviation are displayed in Table 2. Different letters denote significant differences ($p<0.05$) between alloys. Addition of palladium to NiCr and CoCr alloys did not significantly alter the microhardness of the alloys, except the CoPdCr-A where its hardness was approximately 90% of the traditional CoCr alloy. Overall, the Co-based alloys were harder than the Ni-based alloys.

Table 2. Vickers microhardness of the five alloys

| Alloys | Vickers hardness (VHN) |
|---|---|
| NiPdCr | 212 ± 1 A |
| NiCr | 196 ± 2 A |
| CoPdCr-A | 309 ± 23 B |
| CoPdCr-I | 343 ± 15 C |
| CoCr | 355 ± 11 C |

Different letters denote significant ($P$ <0.05) differences exist

# DISCUSSION

Observation of the compositions of the alloys show several elements added to the base elements of Co or Ni and Cr. Molybdenum is added to all five alloys and has been recognized as a solid solution strengthening agent in NiCr and aids corrosion resistance.[16] Silicon is added to both Ni-based alloys. Baran[16] mentions that Si may stimulate precipitate formation, as does aluminum which is found in just the NiCr Argeloy N.P. Star alloy. The CoPdCr alloys contain a small amount of boron, which has been shown to raise the melting range of CoCr causing carbides to be dispersed and distributed within grains rather than precipitated at the grain boundaries.[22] Discovering the effect adding palladium to CoCr and NiCr alloys has on the microstructure formed the basis for this research.

All five alloys presented with a dendritic microstructure. This is in agreement with previous studies that show the etched microstructure of NiCr and CoCr base metal alloys is dendritic in nature.[9,22] As with the vast majority of base metal dental alloys, a lack of grain refining agent suggests a greater likelihood of obtaining a dendritic microstructure. Contrarily, many high noble and noble dental casting alloys contain grain refining elements such as Ru and Ir, resulting in a more equiaxed grain structure.[26]

Comparing the microstructures displayed in Figures 1-15, it is apparent the addition of palladium introduced increased complexity to the microstructure. There appear to be a greater number of precipitates and/or secondary phases in the respective micrographs. For the CoCr system, further addition of alloying elements beyond what is found in the most basic and/or initial CoCr formulations (~60% Co and ~25%Cr) increases the complexity of the alloy microstructure.[22] This is also consistent with the

results of Reclaru et al.[23,24] who showed adding small amounts of noble elements to CoCr increased the complexity of the CoCr microstructure. Specifically, round inclusions rich in Au were introduced when gold was added to the alloys. However, it should be mentioned the solubility of gold in Co is much less than Pd in Co. Yet, when Reclaru et al.[23,24] added platinum, which is more soluble in Co than Au, some Pt-containing precipitates did form despite Pt also appearing in the matrix which was richer in Co and Mo.

The response of the Pd-containing alloys in this study to etching is further proof of the increased complexity as it was relatively easy to over etch the alloys presumably due to areas of different elemental concentration. With the especially heterogeneous microstructure, some areas were much more receptive/reactive to the etchants than other areas. This is coupled with the fact that many Co-based alloys are challenging to etch in the first place[22], which may lead to difficulty with interpretation of the microstructure. The NiCr and Co-containing alloys were etched in a mixture of nitric and hydrochloric acids whereas the NiPdCr alloy was etched in a solution of hydrochloric acid and hydrogen peroxide.

SEM coupled with EPMA is a very valuable tool for metallurgical analysis as one is able to map out elemental concentrations with respect to microstructural features. For NiPdCr and CoPdCr-A, a region of the microstructure imaged with a backscattered electron detector displayed the expected dendritic microstructure. Elemental maps for Co or Ni, Cr, Pd, and Mo were then mapped out with respect to the micrograph. For both alloys, chromium was rather uniformly distributed in the entire microstructure. Although comparison between the two maps may not be valid, it is interesting to note the EPMA

shows the CoPdCr-A alloy possesses relatively lower levels of Cr compared to the NiPdCr alloy (green vs. yellow/red, respectively). This is consistent with the Cr content levels in the alloys as supplied by the manufacturers, that being 20 and 25 wt%, respectively. A greater amount of chromium is generally regarded as resulting in an increased corrosion resistance.[9] The increased Cr content in NiPdCr compared to the CoPdCr alloys may explain why Beck et al.[5] observed increased elemental release in the latter alloys but NiPdCr did not significantly differ from NiCr.

For both the CoPdCr and NiPdCr alloy, microsegregation is apparent. Microsegregation is a nonuniform distribution of alloying elements within a solidification microstructure, or in other words, a chemical nonuniformity exists. Cobalt or nickel and molybdenum tended to be enriched in areas where the amount of palladium tended to be less. Contrarily, palladium rich areas tended to coincide with lesser Co or Ni and Mo. Some precipitates may be evident in both alloys, but more so in the NiPdCr alloy. When viewing the Cr distribution maps, discrete singular areas rich in Cr appear (red in color indicting increased concentration). Coinciding with this tends to be low areas of the other elements. The full composition of these areas, however, was not able to be determined. The segregation of different elements resulting in areas of varying composition supports the results from the corrosion studies mentioned earlier.[4,5]

The solidification of castings produced from CoCr and NiCr-based alloys involves the formation of dendritic regions followed by interdendritic regions which are usually richer in solute and may lead to the segregation mentioned above. Unfortunately no previous studies on the composition of the NiPdCr and CoPdCr alloys exist. However, one study did do EPMA of NiCr and CoCr based dental casting alloys.[28] It showed that

the structure of NiCr casting alloys were comprised of white dendritic regions and darker interdendritic areas consisting of gamma prime and certain eutectic carbide phases. Nickel was fairly constant in concentration across the dendrites but significantly increased in one of the linear eutectic carbide region while silica and carbon were more in the interdendritic region. Molybdenum and manganese were maintained across the sample, but aluminum was concentrated more in the dendritic arm and decreased as the scan approached the interdendritic region. The CoCr alloy was comprised of a grey interdendritic carbide region and black dendritic regions. No significant compositional variation occurred from the dendritic to interdendritic region and on to the grain boundary regions. The chromium and molybdenum concentration was high in the dendritic region. The first solid to form was essentially the nickel-chromium and cobalt-chromium solid solutions, respectively.

The binary phase diagrams for the various alloying elements shows Pd is very soluble in Ni and Co but fairly insoluble in Mo.[29] The binary CoCr and NiCr phase diagrams show extensive solid solubility of chromium in cobalt and nickel, respectively. The melting point of Co, Cr, Mo, Ni, and Pd are 1495, 1863, 2623, 1455, and 1555$^{o}$C, respectively.[29] However, the Co-rich areas of the CoMo, CoPd, and CoCr binary phase diagrams indicate the liquidus line is not appreciably sloped nor depart greatly away from the melting point of Co (1495$^{o}$C). The same holds for Ni.

The crystal structures of pure Co, Cr, Mo, Ni, and Pd at room temperature are hexagonal, bcc, bcc, fcc, and fcc, respectively.[29] Cobalt does exist as an allotrope with transformation from a hexagonal ($\varepsilon$) to fcc ($\alpha$) crystal structure above 422$^{o}$C.[29]

Indexing of the XRD patterns showed that the pattern is mostly related to the major element in the composition, however alloying elements may shift the pattern. For NiCr and NiPdCr, the peaks are reflections of a nickel solid solution with a fcc crystal structure. Alloying with chromium and/or palladium shifted the peaks to lower angles compared to the Ni standard pattern. Between NiCr and NiPdCr, the addition of the Pd, mostly at the expense of Ni, further shifted the peaks to lower angles. The lattice parameters for NiCr and NiPdCr were 0.360 nm and 0.369 nm, respectively, while that of pure Ni is 0.352 nm[29] which means that alloying also increased the lattice parameter of the fcc Ni. For the Co-based alloys, slightly different spectra were obtained when comparing the CoCr to CoPdCr alloys. In the CoPdCr-A and CoPdCr-I alloys, the spectra best matched the ICDD pattern for fcc Co, whereas CoCr alloys, the spectrum best matched the ICDD pattern for hexagonal Co. Palladium may have stabilized the fcc structure to room temperature. For all three Co-based alloys, the peaks are related to cobalt solid solutions and again, as in the NiPdCr alloy, alloying CoCr with palladium shifted the peaks to lower angles compared to the Co standard. The lattice parameter for CoPdCr-A and CoPdCr-I was 0.367 nm and 0.369 nm, respectively, while that of pure Co in an fcc crystal structure is 0.355 nm.[29] Again, alloying increased the lattice parameter of the Co-based alloys.

The increase in lattice parameter for all of the fcc alloys compared to the primary pure metal component (Co or Ni) is not surprising given the atomic radii of the elements are in the following order: Ni (0.162 nm), Co (0.167 nm), Pd (0.179 nm), Cr (0.185 nm), and Mo (0.201 nm).[30] The greater size of the major alloying elements increases the spacing between the atoms compared to the pure Ni or Co crystal.

When viewed the XRD data is viewed in context of the optical microscopy and SEM/EPMA data, a discrepancy appears to arise since only a solid solution was detected via XRD. However, any precipitates or secondary phases believed to be observed in the micrographs mentioned above perhaps were not in enough abundance to be detected with the XRD parameters used in this study.

Comparison of the obtained XRD spectra to the ICDD patterns suggests preferred orientation was observed in all of the alloys. This is detected when the relative intensity of the peaks in the ICDD pattern are not consistent with the relative intensities of the peaks in the specimen. In a textured or preferred orientation, the distribution of crystals is nonrandom whereas a random arrangement of crystals would result in the relative peak intensities observed for the Co or Ni powdered standards. The preferred orientation in these alloys most likely arises due to the casting procedures used for fabricating dental prostheses with growth during solidification occurring along certain planes in addition to areas of the casting solidifying at different rates.[26] Past studies of both dendritic and equiaxed dental casting alloys have also observed preferred orientation in as-cast structures.[26]

When comparing the microhardness of the Pd-containing NiCr and CoCr alloys to their respective counterparts, only a slight effect was observed. The VHN of the CoPdCr-A alloy was significantly lower than that of CoCr, but CoPdCr-I and CoCr were similar. The reason for the difference in hardness between the CoPdCr is not entirely clear, but it may be related to the minor elements, such as W and Ta, that are added in CoPdCr-I that do not appear in CoPdCr since the concentration of the major elements (Co, Cr, Pd, Mo) are pretty similar. For the Ni-based alloys, the mean VHN value of NiPdCr was 212

whereas the mean VHN of NiCr was 196, but the values were not significantly different. Since CoCr and NiCr already contain solid solution strengthening elements, it is probable that the addition of yet another solid solution strengthening element (Pd) did not exert an appreciable effect in microhardness.

# CONCLUSIONS

Conclusions generated from the metallurgical characterization of two palladium-containing CoCr alloys-CoPdCr-A and CoPdCr-I, one palladium-containing NiCr alloy-NiPdCr, and a traditional CoCr and NiCr alloy using optical microscopy, SEM/EPMA, XRD, and Vickers microhardness were:

- All five alloys displayed a dendritic microstructure via optical microscopy, but the Pd-containing alloys possessed a more complex microstructure.
- The microstructures of NiPdCr and CoPdCr-A exhibited microsegregations as detected by SEM/EPMA. Palladium tended to be segregated apart from Mo and Ni or Co. In both alloys, Cr is rather uniformly distributed in the matrix.
- XRD showed that Ni-containing alloys were primarily fcc Ni solid solution. For the Co-based alloys, slightly different spectra were obtained with the traditional CoCr consistent with a hexagonal Co solid solution whereas the CoPdCr alloys best matched the ICDD pattern for fcc Co.
- For Vickers hardness, the Co-based alloys had higher hardnesses than the Ni-based alloys. The incorporation of Pd in CoCr and NiCr had only a slight effect on microhardness.

## REFERENCES


1. American Dental Association (ADA). ADA Positions & Statements: Revised classification system for alloys for fixed prosthodontics. Accessed at: https://www.ada.org/prof/resources/positions/statements/prosthodontics.asp on June 9, 2009.

2. Wataha JC. Alloys for prosthodontic restorations. J Prosthet Dent 2002; 87:351-63.

3. Naylor WP. Introduction to metal ceramic technology. Chicago: Quintessence Pub. Co.; 1992. pp. 27-41.

4. Sarantopoulos DM, Beck KA, Holsen R, Berzins DW. Corrosion of CoCr and NiCr dental alloys alloyed with palladium. J Prosthet Dent. 2011;105:35-43.

5. Beck KA, Sarantopoulos DM, Kawashima I, Berzins DW. Elemental release from CoCr and NiCr alloys containing palladium. J Prosthodont (in press).

6. Huang HH. Effect of chemical composition on the corrosion behavior of Ni-Cr-Mo dental casting alloys. J Biomed Mater. 2002; 60: 458–465.

7. Gil FJ, Sanchez LA, Espias A, Planell JA. In vitro corrosion behaviour and metallic ion release of different prosthodontic alloys. Int Dent J 1999; 49:361-7.

8. Manaranche C, Hornberger H. A proposal for the classification of dental alloys according to their resistance to corrosion. Dent Mater 2007; 23:1428-37.

9. Wylie CM, Shelton RM, Fleming GJ, Davenport AJ. Corrosion of nickel-based dental casting alloys. Dent Mater. 2007;23:714-23.

10. Baran G. Oxidation kinetics of some Ni-Cr alloys. J Dent Res. 1983;62:51-5.

11. Baran GR. Phase changes in base metal alloys along metal-porcelain interfaces. J Dent Res. 1979;58:2095-104.

12. Anusavice KJ. Phillips' science of dental materials. 11$^{th}$ ed. Philadelphia:WB Saunders; 2003. pp. 120-121.

13. Vander Voort GF. Optical microscopy. In ASM Handbook, Volume 9: Metallography and Microstructures. Vander Voort GF volume editor. Materials Park, OH:ASM International; 1985. pp. 71-88.

14. Exner HE. Scanning electron microscopy. In ASM Handbook, Volume 9: Metallography and Microstructures. Vander Voort GF volume editor. Materials Park, OH:ASM International; 1985. pp. 89-102.

15. Cullity BD. Elements of x-ray diffraction. 2nd ed. Reading, MA:Addison-Wesley Publishing Company, Inc.; 1978.

16. Baran GR. The metallurgy of Ni-Cr alloys for fixed prosthodontics. J Prosthet Dent. 1983;50:639-50.

17. Baran G. Auger chemical analysis of oxides on Ni-Cr Alloys. J Dent Res. 1984;63:76-80.

18. Baran GR. Oxide compounds on Ni-Cr alloys. J Dent Res 1984;63:1332-4.

19. Lin HY, Bowers B, Wolan JT, Cai Z, Bumgardner JD. Metallurgical, surface, and corrosion analysis of Ni-Cr dental casting alloys before and after porcelain firing. Dent Mater. 2008;24:378-85.

20. Huget EF, Dvivedi N, Cosner Jr. HE. Properties of two nickel-chromium crown-and-bridge alloys for porcelain veneering. JADA. 1977;94:87-90.

21. Roach MD, Wolan JT, Parsell DE, Bumgardner JD. Use of x-ray photoelectron spectroscopy and cyclic polarization to evaluate the corrosion behavior of six nickel-chromium alloys before and after porcelain-fused-to-metal firing. J Prosthet Dent. 2000;84:623-34.

22. Asgar K, Allan FC. Microstructure and physical properties of alloys for partial denture castings. J Dent Res. 1968;47:189-97.

23. Reclaru L, Lüthy H, Eschler PY, Blatter A, Loeffel O, Zurcher MH. Cobalt-chromium dental alloys enriched with precious metals. European Cells and Materials 2004;7(Supplement 2):51-52.

24. Reclaru L, Lüthy H, Eschler PY, Blatter A, Susz C. Corrosion behaviour of cobalt-chromium dental alloys doped with precious metals. Biomaterials. 2005;26:4358-65.

25. Vermilyea SG, Cai Z, Brantley WA, Mitchell JC. Metallurgical structure and microhardness of four new palladium-based alloys. J Prosthodont. 1996;5:288-94.

26. Brantley WA, Cai Z, Foreman DW, Mitchell JC, Papazoglou E, Carr AB. X-ray diffraction studies of as-cast high-palladium alloys. Dent Mater. 1995;11:154-60.

27. Brantley WA, Cai Z, Papazoglou E, Mitchell JC, Kerber SJ, Mann GP, Barr TL. X-ray diffraction studies of oxidized high-palladium alloys. Dent Mater. 1996;12:333-41.

28. Lewis AJ. An electron microprobe investigation of the extent of microsegregation occurring in base metal dental casting alloys. Australian Dental Journal. 1979;24:171-3.

29. ASM International. ASM Handbook, Volume 03: Alloy Phase Diagrams. Baker H, Okamoto H volume editors. Materials Park, OH:ASM International; 1992.

30. http://environmentalchemistry.com accessed on April 8, 2011.